Synthetic *in vitro* transcribed lncRNAs (SINEUPs) with chemical modifications enhance target mRNA translation

Naoko Toki[1,2] (iD), Hazuki Takahashi[1,2] (iD), Silvia Zucchelli[3], Stefano Gustincich[4,5] (iD) and Piero Carninci[1,2] (iD)

1 Laboratory for Transcriptome Technology, RIKEN Center for Integrative Medical Sciences, Yokohama, Japan
2 Functional Genomics Laboratory, Graduate School of Medical Life Science, Yokohama City University, Yokohama, Japan
3 Department of Health Sciences, Center for Autoimmune and Allergic Diseases (CAAD) and Interdisciplinary Research Center of Autoimmune Diseases (IRCAD), University of Piemonte Orientale (UPO), Novara, Italy
4 Department of Neuroscience and Brain Technologies, Istituto Italiano di Tecnologia (IIT), Genova, Italy
5 Area of Neuroscience, International School for Advanced Studies (SISSA), Trieste, Italy

Chemically modified mRNAs are extensively studied with a view toward their clinical application. In particular, long noncoding RNAs (lncRNAs) containing SINE elements, which enhance the translation of their target mRNAs (i.e., SINEUPs), have potential as RNA therapies for various diseases, such as haploinsufficiencies. To establish a SINEUP-based system for efficient protein expression, we directly transfected chemically modified *in vitro* transcribed (mIVT) SINEUP RNAs to examine their effects on target mRNA translation. mIVT SINEUP RNAs enhanced translation of *EGFP* mRNA and endogenous target *Sox9* mRNA in both cultured cells and a cell-free translation system. Our findings reveal the functional role of RNA modifications in SINEUPs and suggest several broad clinical applications of such an RNA regulatory system.

Keywords: enhancement of endogenous target mRNA translation; *in vitro* transcribed RNA; nucleic acid-based therapeutics; RNA modification

The advancement of genomics technologies revealed that an emerging class of long noncoding RNAs (lncRNAs) [1], which constitute the majority of types of transcripts and do not encode proteins [2,3], plays key regulatory roles in the physiology of normal cells, the development of diseases including cancer [4] and neurodegenerative diseases [5]. The discovery of increasing numbers of functional lncRNAs has prompted novel therapeutic applications, including the treatment of human genetic diseases. A functional lncRNA transcribed from the antisense strand of *Uchl1* mRNA contains an inverted SINEB2 element and upregulates the translation of its sense strand *Uchl1/Park5* mRNA in mouse dopaminergic neuronal cells [6]. This lncRNA was the first in a large class of antisense lncRNAs, named 'SINEUPs', because they contain an embedded inverted SINEB2 element that acts as an effector domain (ED) to mediate UPregulation of the translation of the target mRNA; the target specificity is determined by the antisense RNA region, the binding domain (BD) [7].

SINEUP-based upregulation systems occur in various cell types [7] and vertebrates including humans,

mice, and fish [8–12]. We have focused on broadening the scope of SINEUP-based upregulation systems so that they can be applied to direct nucleic acid-based therapeutics [5,13,14]. We consider that SINEUPs might be therapeutically useful for various disorders caused by insufficient protein production [10] or haploinsufficiency. At least 300 genes are linked to haploinsufficiencies [15], for which more than 3000 genes are predicted as possible therapeutic candidates [16]. In one SINEUP proof-of-concept study, the target is the medaka *cox7B* gene; mutations in the human homolog subunit 7B of cytochrome *c* oxidase (*COX7B*), the product of which is a component of the mitochondrial respiratory chain, are responsible for the disease microphthalmia with linear skin lesions. To rescue a medaka model of microphthalmia with linear skin lesions, we introduced synthetic *in vitro* transcribed (IVT) SINEUP-cox7B, designed against endogenous *cox7B* mRNA. IVT SINEUP-cox7B enhanced COX7B protein production and consequently rescued eye and brain size in cox7B morphants [12]. Whether direct administration of SINEUP RNA effectively enhances protein production in cell types or species other than medaka is unknown. Here, we successfully developed synthetic, chemically modified IVT (mIVT) SINEUPs that upregulated the translation of target enhanced green fluorescent protein (*EGFP*) mRNA and endogenous target sex-determining region Y (SRY)-box 9 (*Sox9*) mRNA in cultured cells. In addition, mIVT SINEUP RNA successfully upregulated EGFP production in a HeLa extract cell-free translation system, which contains the SINEUP-specific RNA-binding proteins (RBPs) HNRNPK and PTBP1 [17].

The current study improves our understanding of the system through which mIVT SINEUP RNAs regulate both exogenous and endogenous targets in specific cell types and in a cell-free system. Therefore, our current findings support nucleic acid-based therapeutics as additional tools for gene therapy of human disorders due to insufficient protein production.

Materials and Methods

Cell culture

Human embryonic kidney (HEK 293T/17) cells, human hepatocellular carcinoma (HepG2) cells, and mouse hepatocellular carcinoma (Hepa1–6) cells were obtained from ATCC (Manassas, VA, USA) and cultured in Dulbecco's modified Eagle's medium $(1\times)$ + GlutaMAX-1 (Gibco) supplemented with 10% FBS (Sigma, St. Louis, MO, USA) and 1% penicillin–streptomycin (Wako, Osaka, Japan) at 37°C, 5% CO_2.

Plasmids and constructs

The pEGFP-C2 plasmid was purchased from Clontech Laboratories (Takara Bio USA, Mountain View, CA, USA). The pCS2+_SINEUP-GFP plasmid was generated in a previous study [17]. The BD of SINEUP targeting GFP, Δ5′-32 nt, has a deletion of 28 bases from the 5′ end of the original 60 nt SINEUP-GFP and corresponds to the mRNA positions −28 to +4 (see Fig. 1B in [18]). The pcDNA3.1_EGFP plasmid was constructed by cloning a fragment encoding full-length EGFP (−40 bp to the stop codon) from the plasmid pEGFP-C2 into pcDNA3.1(–) (Thermo Fisher Scientific, Waltham, MA, USA). The SINEUP targeting mouse *Sox9* (named miniSINEUP-Sox9) contained a BD that overlapped mouse *Sox9* mRNA (in antisense orientation) and the control without BD (named miniSINEUP-Random; Rd) contained a random sequence instead of the Sox9-BD, those have an ED containing an inverted SINEB2 sequence from mouse *AS-Uchl1* RNA, were cloned into the pCS2+ vector (Fig. S1).

IVT RNAs

SINEUP RNAs were synthesized by using mMES-SAGE mMACHINE SP6 Transcription Kit (Thermo Fisher Scientific) according to the manufacturer's instructions and as modified from a protocol [19] by using the following nucleotide modifications: modified nucleotides (all from TriLink, San Diego, CA, USA; final concentration, 7.5 mM): CTP was replaced with 5-methylcytidine-5′-triphosphate (m^5C), and UTP was replaced with pseudouridine-5′-triphosphate (Ψ) or N1-methylpseudouridine-5′-triphosphate (N^1mΨ). The regents were mixed with 40 ng·μL^{-1} (final concentration) of linearized SINEUP plasmid. A poly-A tail was added to the IVT RNA (1–10 μg per reaction) by using *Escherichia coli* poly(A) polymerase (5000 U·mL^{-1}; catalog no. M0276; New England Biolabs, Tokyo, Japan) at 37 °C for 30 min; resulting mIVT RNAs were extracted by using RNeasy Mini kit (Qiagen, Tokyo, Japan).

Plasmid and RNA transfection

HEK293T/17 cells were plated into 12-well plates $(1 \times 10^5$ cells per well), followed 24 h later by transfection of plasmid or RNA (IVT, or mIVT). To detect EGFP, 1380 ng SINEUP-GFP plasmid or 720 ng (m) IVT *SINEUP-GFP* RNA was cotransfected with 300 ng pEGFP-C2 in each well by using Lipofectamine 2000 (Invitrogen, Waltham, MA, USA) with OptiMEM $(1\times)$ Reduced Serum Medium (Gibco). The cells were harvested at 24 h after transfection. To detect endogenous SOX9, HEK293T/17 cells were
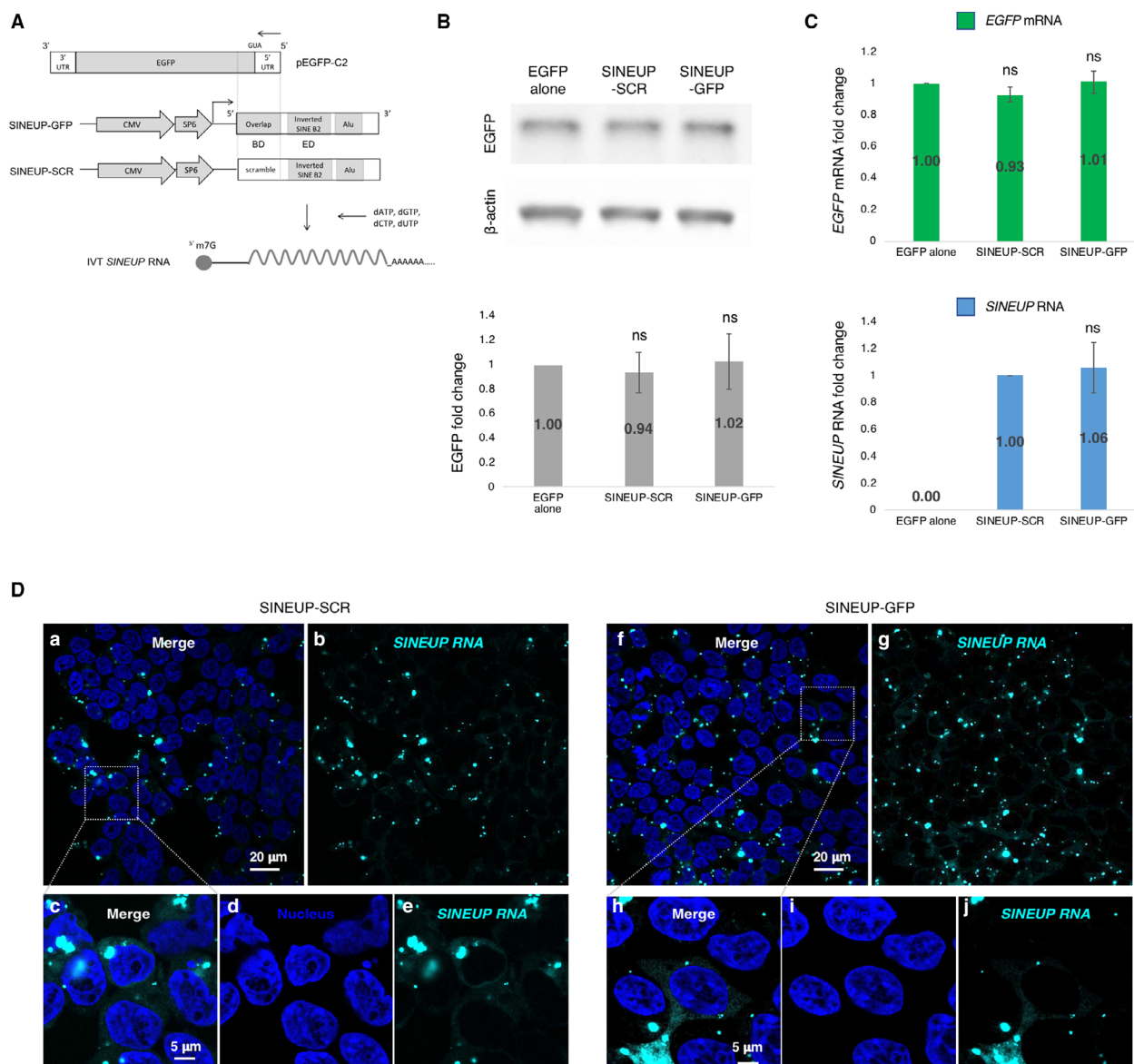
Fig. 1. Transfection of IVT SINEUP RNA into HEK293T/17 cells. (A) Schematic representation of the SINEUP constructs. SINEUP-GFP contains an overlapping region with *EGFP* mRNA as a BD and inverted SINEB2 element as an ED. SINEUP-SCR contains a scrambled and thus nonfunctional sequence from the BD of SINEUP-GFP. (B) Translational upregulation of EGFP by cotransfection of EGFP plasmid and IVT SINEUPs. Representative western blot images showing the effect of IVT SINEUPs on the level of EGFP as detected by using an anti-GFP rabbit polyclonal antibody. Data are shown as means ± SD of at least three independent experiments. ns, not significant (two-tailed Student's *t*-test). (C) Quantification of *EGFP* mRNA and the IVT SINEUP RNA levels after cotransfection of EGFP plasmid and IVT SINEUPs. ns, not significant (two-tailed Student's *t*-test). Data are shown as means ± SD from at least three independent experiments. (D) Subcellular localization of IVT SINEUPs. Bars, 20 μm (a, f), 5 μm (c, h).

plated into 12-well plates (1×10^5 cells), followed 24 h later by transfection of 2 μg miniSINEUP-Sox9 plasmid or 100 ng of mIVT *miniSINEUP-Sox9* RNA per well. Cells were harvested at 24 and 48 h after plasmid transfection and at 24 h after mIVT transfection.

Cell-free translation

Rabbit reticulocyte lysate (RRL) was purchased from Promega (Madison, WI, USA) (catalog no. L4610, TNT Coupled Reticulocyte Lysate System), and a lysate of HeLa cells (catalog no. 8881, 1-Step Human Coupled IVT Kit—DNA) was purchased from

Thermo Fisher Scientific. *In vitro* translation was performed according to the manufacturer's protocol. Briefly, for each reaction, 400 ng of SINEUP plasmid or 200 ng of (m)IVT SINEUP RNA was mixed with 120 ng pcDNA3.1_EGFP. The mixture was incubated for 90 min at 30 °C. Protein expression was measured by western blotting.

Western blotting

Transfected cells were lysed in Cell Lysis Buffer (Cell Signaling Technology, Danvers, MA, USA) and incubated at 4 °C for 1 h. Cell lysates were loaded on a 10% precast polyacrylamide gel (Bio-Rad, Hercules, CA, USA), separated by SDS/PAGE, and transferred to a nitrocellulose membrane (Amersham, Chicago, IL, USA). All primary and secondary antibodies were used at 1 : 1000 dilution. To detect EGFP, anti-GFP mouse monoclonal antibody (clone JL-8; catalog no. 632380; Clontech, Chicago, IL, USA) in the RRL cell-free system and anti-GFP rabbit polyclonal antibody (catalog no. A-6455; Thermo Fisher Scientific) in a lysate of HeLa cells and in culture cells were used. To detect RBPs, the primary antibodies, anti-hnRNP K mouse monoclonal antibody [3C2]-ChIP Grade (ab39975; Abcam), and anti-PTBP1 mouse monoclonal antibody (32-4800; Thermo Fisher Scientific) were used. To detect endogenous SOX9, anti-Sox9 rabbit monoclonal antibody (clone EPR14335; catalog no. ab185230; Abcam) was used.

The membranes were incubated with primary antibodies at 4 °C overnight, followed by incubation for 45 min at room temperature with secondary anti-mouse IgG, or anti-rabbit IgG conjugated with HRP (Dako, Tokyo, Japan). Bands were visualized by using ECL Detection Reagent (Amersham). As a control, primary mouse anti-β actin monoclonal antibody (Sigma-Aldrich) and secondary HRP-conjugated anti-mouse IgG (Dako) were used. Bands were detected by using the quantification analysis module and chemiluminescence application protocol of the Fusion Solo S System (Vilber-Lourmat, Osaka, Japan).

RNA extraction and quantification

Total RNA was extracted by using RNeasy Mini kit (Qiagen), followed by DNase I treatment (TURBO DNA-free kit; Invitrogen). cDNA was synthesized by using PrimeScript 1st Strand cDNA Synthesis kit (Takara), and quantitative real-time PCR analysis was performed by using SYBR Premix Ex *Taq* II (Takara) in a model 7900HT Fast Real-Time PCR System (Applied Biosystems, Foster City, CA, USA).

Thermocycling conditions consisted of an initial 30 s at 95 °C, 40 cycles comprising 95 °C for 5 s, and 60 °C for 30 s, followed by melting curve analysis.

RNA fluorescence *in situ* hybridization

RNA fluorescence *in situ* hybridization (FISH) was performed as previously described [17]. Briefly, cells were fixed in 4% paraformaldehyde (Wako) and permeabilized in 0.5% Triton X-100 (Sigma-Aldrich) at room temperature for 5 min. RNA was hybridized with fluorescently labeled (Quasar 570 for SINEUP RNAs and Quasar 670 for *EGFP* mRNA) RNA FISH probes designed by using Stellaris RNA FISH Designer (Biosearch Technologies, Novato, CA, USA; Tables S1 and S2) and incubated overnight at 37 °C. Cells were washed and imaged by using a model SP8 (Leica, Wetzlar, Germany) confocal microscope.

Results

IVT *SINEUP-GFP* RNA failed to increase EGFP synthesis

Previously, we found that colocalization of target mRNA and SINEUP RNA in the cytoplasm is required for upregulation of target mRNA translation [17]. We therefore hypothesized that direct transfection of IVT SINEUP RNA into the cytoplasm would enhance protein production more than transfection of SINEUP plasmid, which requires the export of RNA transcribed in the nuclei. To test the efficiency of translational upregulation by using IVT SINEUPs, we transfected IVT RNA into HEK293T/17 cells, with EGFP plasmid as a target sense transcript. IVT *SINEUP-GFP* RNA contains a BD designed to target EGFP mRNA (Fig. 1A), whereas IVT *SINEUP-SCR* RNA was designed as a negative control and contains a scrambled, nonfunctional EGFP BD. Transfection of IVT *SINEUP-GFP* did not stimulate the translation of EGFP (Fig. 1B), although, consistent with previous studies, *EGFP* mRNA and SINEUP levels did not differ among the cells (Fig. 1C).

In RNA FISH, most of the IVT SINEUP RNAs aggregated into intense spots within cells, or it was difficult to detect IVT SINEUP RNAs at all (Fig. 1D,e, j). These findings suggested that IVT SINEUP RNAs were partially degraded immediately after transfection and were detected as RNA fragments or were not present in sufficient quantities to adequately colocalize with *EGFP* mRNA. Consequently, EGFP translation was not upregulated.
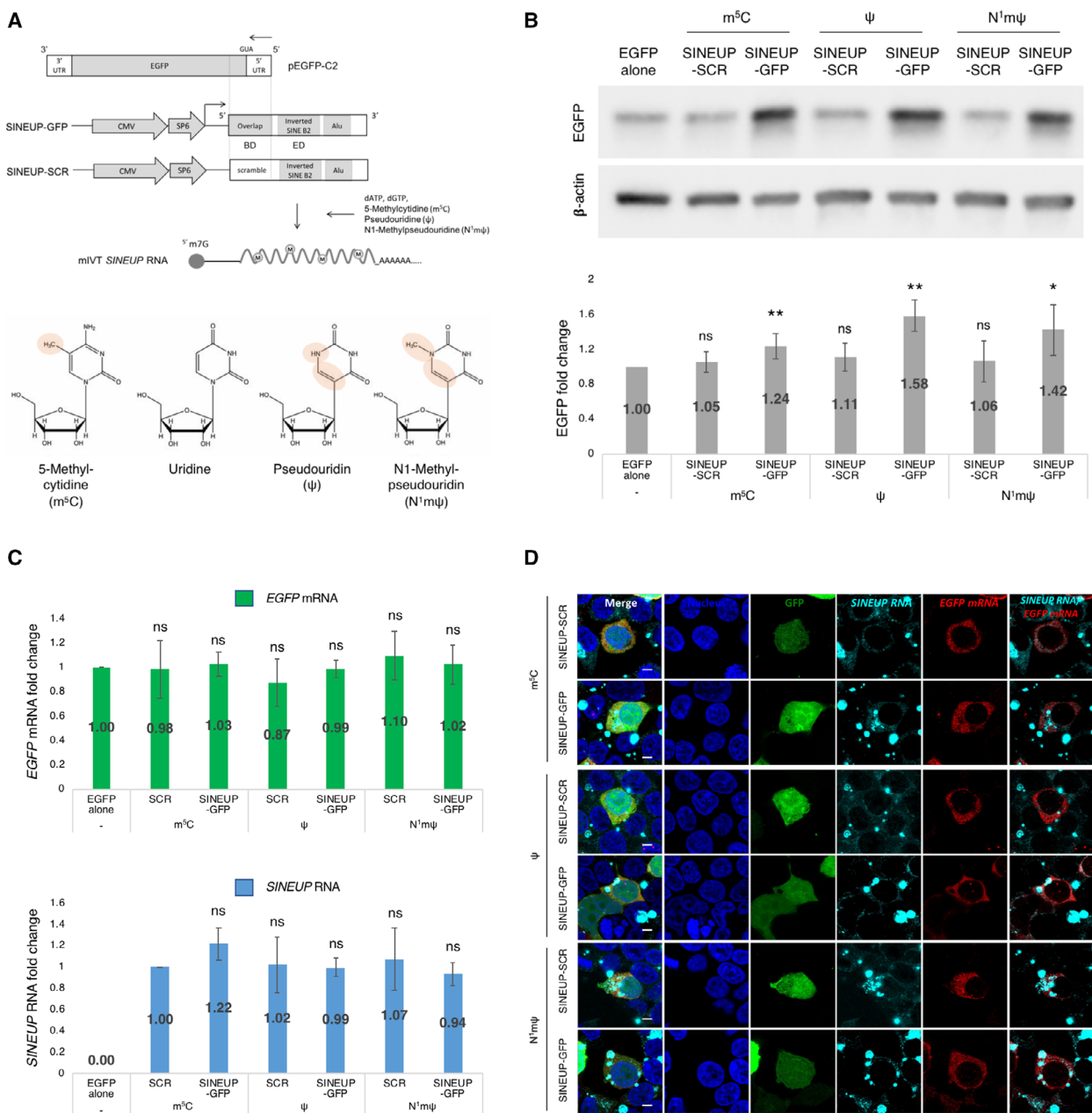
Fig. 2. Transfection of IVT *SINEUP-GFP* RNA containing chemically modified nucleotides into HEK293T/17 cells. (A) Schematic representation of nucleotide-modified SINEUPs. The nucleotide dCTP was replaced with m^5C, and dUTP was replaced with either Ψ or $N^1m\Psi$. The chemical structure models of modified nucleotides are adapted from reference [26]. (B) Translational upregulation of EGFP by cotransfection of EGFP plasmid and mIVT SINEUPs. The images shown are representative of western blots indicating the effect of mIVT SINEUPs on the EGFP level as detected by using an anti-GFP rabbit polyclonal antibody. Upregulation of EGFP levels was measured in at least three independent experiments. Data are shown as means $\pm$ SD. $**P < 0.01$, $*P < 0.05$, ns, not significant (two-tailed Student's *t*-test). (C) Quantification of *EGFP* mRNA and mIVT SINEUP RNA levels after cotransfection of EGFP plasmid and mIVT SINEUPs. Data are shown as means $\pm$ SD from at least three independent experiments. ns, not significant (two-tailed Student's *t*-test). (D) Subcellular distribution of mIVT SINEUPs modified with m^5C, Ψ, or $N^1m\Psi$ after cotransfection with EGFP plasmid. Bar, 5 μm. Figure modified from reference [26].

IVT SINEUP RNAs in cells need to be stabilized through nucleotide modification

Because RNA FISH experiments showed that IVT SINEUPs were likely aggregated after transfection into cells, we hypothesized that stabilization of IVT *SINEUP-GFP* was needed to enhance *EGFP* mRNA translation. RNA transcripts can be stabilized by modified nucleotides, such as m^5C [20,21], Ψ [22,23], or $N^1m\Psi$ [24–26], and these modifications contribute to efficient translation. We therefore synthesized mIVT SINEUP RNAs in which all C or U were replaced with the modified forms and transfected them, together with EGFP plasmid, directly into HEK293T/17 cells (Fig. 2A). All mIVT *SINEUP-GFPs* increased EGFP production compared with the control (EGFP alone and mIVT *SINEUP-SCRs*; Fig. 2B), without affecting *EGFP* mRNA levels (Figs. 2C, Fig. S2A).

We previously found that *SINEUP-GFP* RNAs localized both in the nucleus and in the cytoplasm when pEGFP-C2 and SINEUP-GFP plasmids were cotransfected [17]. We now found that (m)IVT *SINEUP-GFP* localized in the cytoplasm regardless of EGFP plasmid transfection (Fig. 2D, Fig. S3A). Upregulation of *EGFP* mRNA translation did not significantly affect *EGFP* mRNA levels (Fig. 2C, Fig. S2A). Notably, the RNA levels of mIVT SINEUP RNAs were more than 1.5-fold greater than those of IVT SINEUP RNAs (Fig. S2B), implying that these modified nucleotides contributed not only to EGFP upregulation but also to the stabilization of SINEUPs in cells.

## mIVT SINEUPs contribute to EGFP upregulation with SINEUP-binding proteins

We used cell-free translation systems to observe SINEUP upregulation activity separately from RNA stabilization. None of the SINEUP RNAs tested upregulated EGFP in RRL (Fig. 3A), whereas mIVT SINEUPs with Ψ and $N^1m\Psi$- upregulated EGFP in HeLa cell lysate (Fig. 3B). This result suggests that modified nucleotides contribute to the upregulation of EGFP in cell-free system, implying that the expression of cellular components, including RBPs, is important for SINEUP activity [17]. Indeed, the SINEUP RBPs PTBP1 and HNRNPK were expressed at lower levels, approximately 0.2- and 0.5-fold, respectively, in RRL compared with HEK293T/17 cell lysate, which did not show upregulation of EGFP (Fig. 3C–E). These findings suggest that PTBP1 and HNRNPK may have a role in the SINEUP-based upregulation of translation.

mIVT SINEUPs enhance endogenous SOX9 target protein production

To test whether SINEUPs can increase production of endogenous target proteins, we focused on sex-determining region Y (SRY)-box 9 (SOX9) protein; this transcription factor regulates cell differentiation, development, and gene expression in several tissues and organs in vertebrates [27]. In addition, SOX9-positive cells in adult liver can regenerate as hepatocytes after injury [28,29]. Because SINEUPs ultimately are to be used in therapeutic applications, small but still functional SINEUPs are desirable [7]. We therefore designed the miniSINEUP-Sox9 plasmid, in which the BD (−31/+4) overlapped the mouse *Sox9* mRNA and miniSINEUP-Rd plasmid, in which contains a random sequence, nonbinding domain instead of the Sox9-BD, those contained the inverted SINEB2 ED from *AS-Uchl1* RNA (Fig. 4A, Fig. S1). We then transfected these plasmids into HepG2 and Hepa 1–6 cells to examine enhancement of SOX9 protein production. Cells transfected with the miniSINEUP-Sox9 plasmid showed an approximately 1.5-fold upregulation of SOX9 protein compared with the control (no SINE-UPs) at both 24 and 48 h after transfection in HepG2 cells and at 24 h after transfection in Hepa 1–6 cells (Fig. 4B). In addition, the SINEUP RBPs PTBP1 and HNRNPK were expressed in both HepG2 and Hepa 1–6 cells, at no lower than 0.6 times the level in HEK293T/17 cells (Fig. S4A–C). Consistent with

Fig. 3. EGFP upregulation in cell-free translation systems. (A, B) Cell-free translation systems using (A) RRL and (B) HeLa cell lysate. EGFP expression was detected by using (A) anti-GFP mouse monoclonal or (B) anti-GFP rabbit polyclonal antibodies and quantified by western blot analysis. EGFP expression levels were normalized to that of β-actin. Fold induction of EGFP was calculated relative to the number of cells incubated with each SINEUP transcript: that is, transcribed from pCS2+ vector (pCS2+); IVT SINEUP; and modified with m^5C, Ψ, or $N^1m\Psi$. Data are shown as means ± SD of at least three independent experiments. *$P < 0.05$; ns, not significant (two-tailed Student's *t*-test). (C–E) SINEUP RBPs in cell-free lysates compared with HEK293T/17 cells. Images shown are representative western blots of (C) RBPs in the cell-free lysate compared with HEK293T/17 cell lysate. The protein levels of the SINEUP RBPs (D) PTBP1 and (E) HNRNPK were normalized to that of β-actin. Fold change of protein levels is shown as the means ± SD of at least three independent experiments. ***$P < 0.001$, ns, not significant (two-tailed Student's *t*-test).
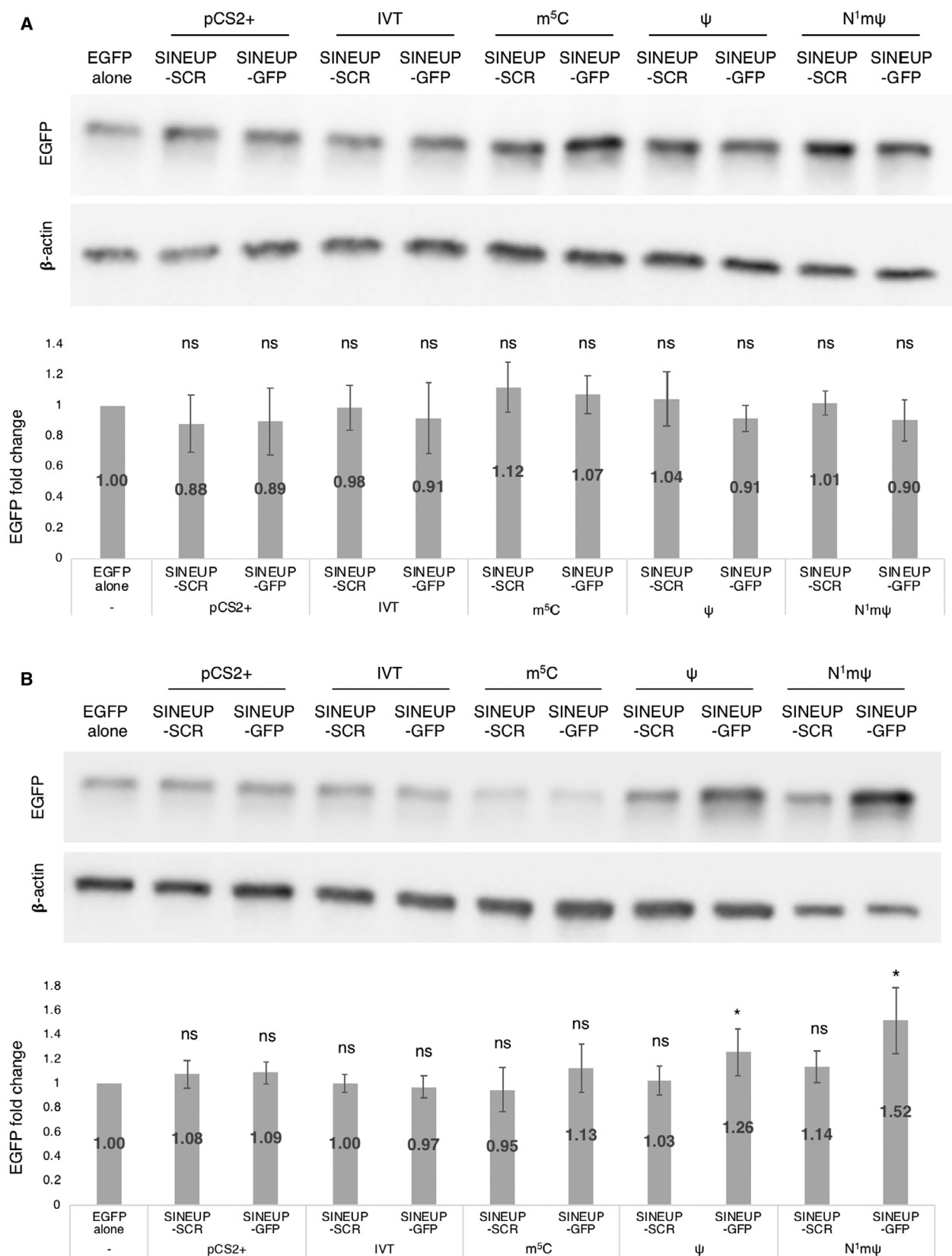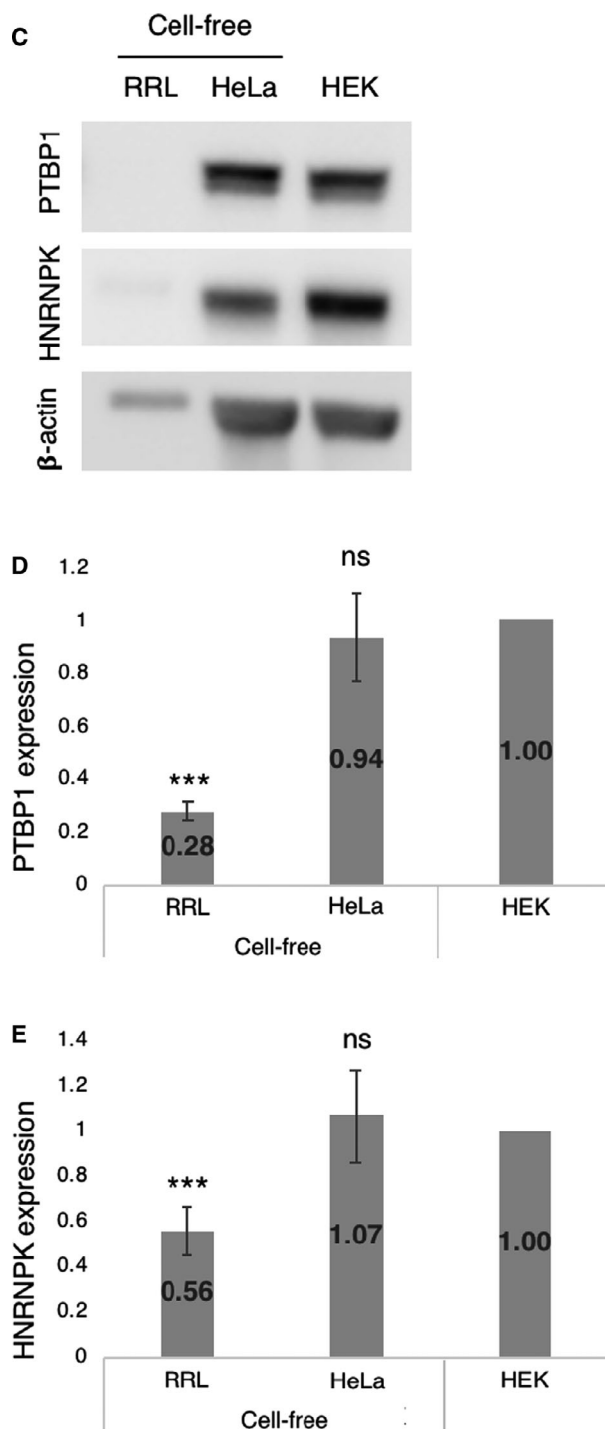
Fig. 3. (Continued)

EGFP study regarding *EGFP* mRNA, endogenous *Sox9* mRNA levels did not change in SINEUP-transfected cells (Fig. 4C). Together, these findings show that miniSINEUP-Sox9 can effectively increase endogenous SOX9 protein levels.

We next tested the efficiency of translational upregulation when mIVT *miniSINEUP-Sox9* containing m^{5}C, Ψ, or N^{1}mΨ was used (Fig. 5A) in HepG2 cells. Similar to the miniSINEUP-Sox9 plasmid, mIVT *miniSINEUP-Sox9* RNAs with Ψ and N^{1}mΨ showed approximately 1.5-fold upregulation of SOX9 protein compared with the control (no mIVT SINEUPs; Fig. 5B). Consistent with the results of plasmid transfection, the endogenous *Sox9* mRNA level was not affected by mIVT miniSINEUP RNAs (Fig. 5C). This result implies that nucleotide modifications might contribute to the stabilization of *miniSINEUP-Sox9* RNA to enhance the SOX9 protein level in HepG2 cells.

Discussion

Synthetic IVT RNAs have diverse potential applications as a new class of druggable tools based on nucleic acid therapeutics. Here, we demonstrated an efficient approach to enhance target protein production through direct transfection of synthetic chemically modified *SINEUP* RNAs. In this study, IVT SINE-UPs with nucleotide modifications were stabilized in cells and increased the EGFP level both in a cell-free translation system and in cultured cells. Using cell-free systems, we found that mIVT SINEUPs upregulated EGFP in HeLa cell lysate but not in RRL. Future studies are needed to assess whether chemical nucleotide modifications of IVT SINEUPs contribute not only to RNA stabilization but also to the interaction with SINEUP-binding proteins, which might be necessary for enhancing translation of the target mRNAs.

The modified nucleotides that we used in this study were chosen not only for their ability to stabilize the target transcripts but also for their importance in several regulation systems. The modified nucleotide m^{5}C stabilizes tRNA [30], aids accurate processing of ncRNA [31], affects the subcellular localization of transcripts [32], and is involved in the regulatory function of lncRNA [33]. In our current study, although m^{5}C-containing mIVT SINEUPs were more stable than IVT SINEUP*s* (Fig. S2B), m^{5}C- did not enhance target protein production (Figs 3B and 5B). Given that RNA modifications change the binding affinities of RBPs [32,34], some positions of m^{5}C residues in mIVT SINE-UPs likely diminished their binding to RBPs, which is important for the localization and translational regulation by SINEUPs and warrants further study.

The modified uridine residue Ψ contributes to mRNA stability, intracellular transcript localization [22], and enhancement of mRNA translation through diminishing protein kinase RNA-activated (PKR) activation [23], and is linked to translation accuracy [35].
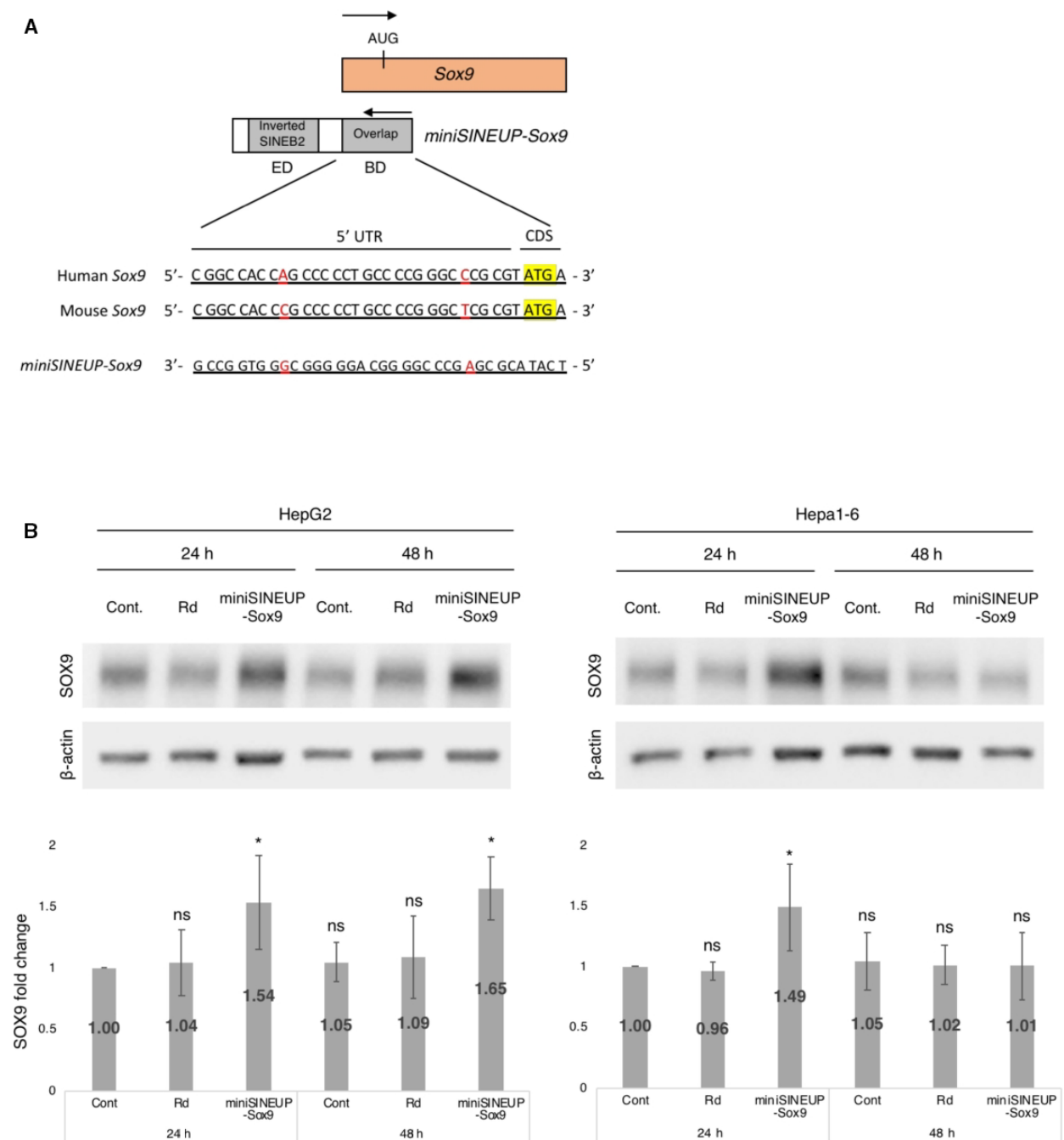
Fig. 4. *miniSINEUP-Sox9* for endogenous target transfected into HepG2 and Hepa 1–6 cells. (A) Schematic representation of the *miniSINEUP-Sox9* construct. *miniSINEUP-Sox9* contains an overlapping region with *Sox9* mRNA as a BD and the inverted SINEB2 motif from *AS-Uchl1* RNA as an ED. (B) Translational upregulation of SOX9 protein due to transfection of *miniSINEUP-Sox9* or *miniSINEUP-Random* (Rd), which contains a random sequence instead of the BD in *miniSINEUP-Sox9*. Image shown is a representative western blot illustrating the effect of SINEUPs on the SOX9 protein level. Quantification of SOX9 levels compared with nontransfected cells (Cont.) is shown as means ± SD of at least 3 independent experiments. *$P < 0.05$; ns, not significant (two-tailed Student's *t*-test). (C) Quantification of *Sox9* mRNA and miniSINEUP RNA levels after transfection with SINEUP plasmid. ns, not significant (two-tailed Student's *t*-test). Data are shown as means ± SD of at least three independent experiments.
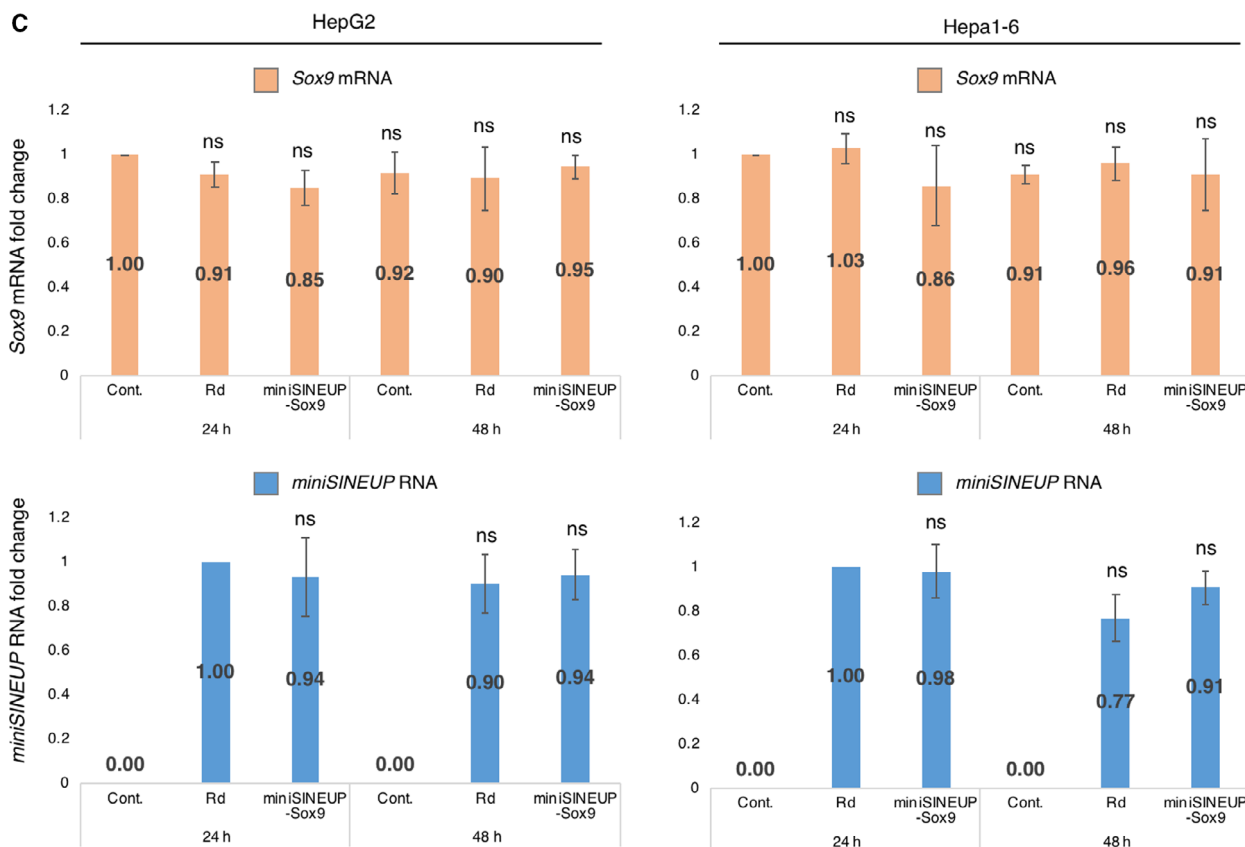
Fig. 4. (Continued)

In addition, RNA duplexes are stabilized when U is replaced with Ψ, leading to the formation of stable Ψ-A, Ψ-G, Ψ-U, and Ψ-C pairs [22]. $N^1m\Psi$ enhances mRNA translation by increasing ribosome density [24] and reduces immunogenicity [25]. Together, these reports suggest that multiple nucleotide modification of RNA has diverse functional possibilities that act through increasing mRNA stability and regulating translation. This knowledge has led to the development of modified mRNA-based approaches for immune cancer therapy and vaccination [36]. In addition to these current nucleic acid-based therapies, SINEUPs have the potential to be used to increase protein production as a biotechnological tool [37], for recombinant antibodies [9,38] and in gene therapy [12], including for diseases that are currently difficult to treat. Adding to current DNA-based gene therapy approaches, RNA-based druggable systems have several advantages, including avoiding the risk of foreign gene integration into the host genome and insertional mutations that may lead to unexpected adverse side effects. In particular, mIVT SINEUP RNAs can be used as an RNA-based drug tool to stimulate only specific target mRNA translation without altering the endogenous mRNA itself, reducing the incidence of unexpected immune responses because of the introduction of modified nucleotides into IVT SINEUPs. Furthermore, mIVT SINEUP RNAs can easily be scaled down to the smallest functional SINEUP RNA, which can then be transported to the target organs with minimal invasive effects to the host. Although how SINEUP RNAs are modified naturally in living cells remains unknown, such modifications, which are missing from IVT transcripts, are likely necessary for SINEUP functions, given that nucleotide modifications can influence protein–RNA interactions and the subcellular distribution of RNAs [39]. The specific modified nucleotides we used in this study are known to alter mRNA secondary structure and thus the half-life and translation efficiency of these transcripts [26]. Ascertaining the importance of the positions of modified nucleotides and improving our understanding of how— and which—modified nucleotides contribute to protein upregulation are crucial goals, and continued research into these modifications of SINEUPs and their application as druggable tools is necessary.

In conclusion, we here showed that synthetic, chemically modified IVT SINEUPs have potential as an efficient, protein-producing tool in nucleic acid-based
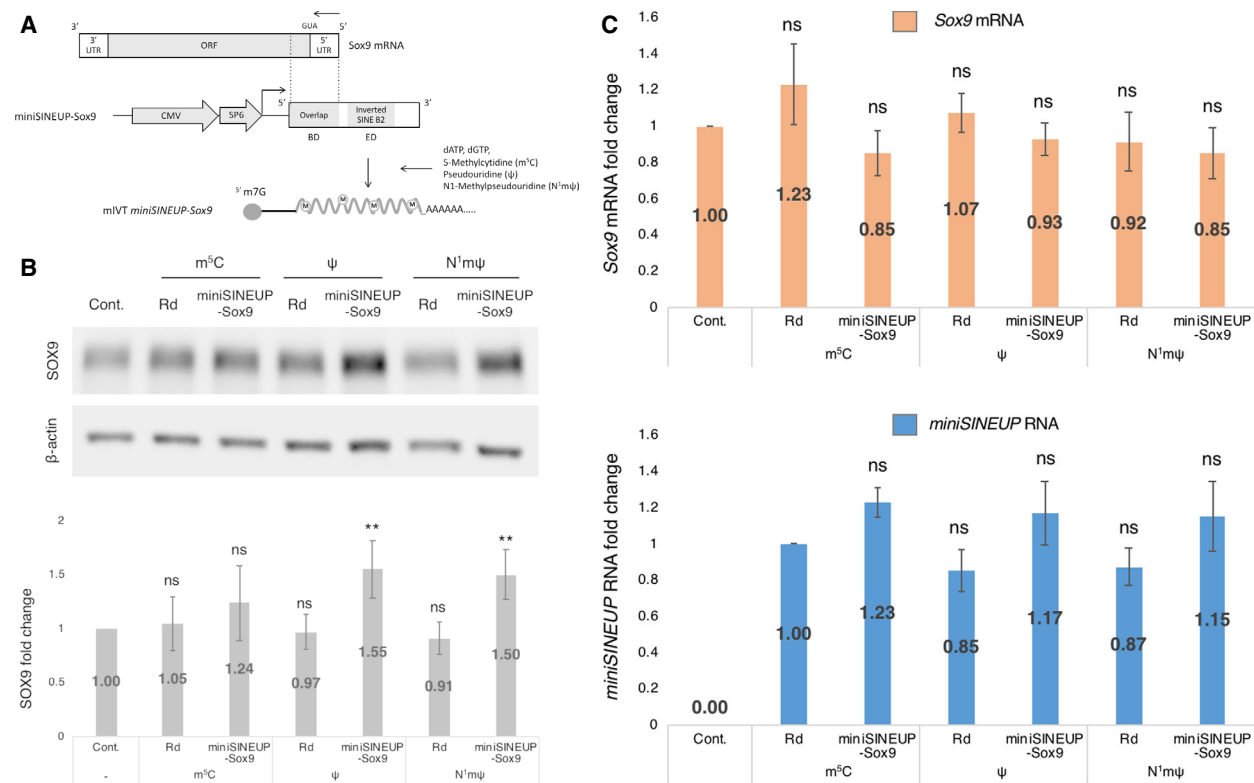
Fig. 5. Transfection of mIVT *miniSINEUP-Sox9* in HepG2 cells. (A) Diagram of nucleotide modifications in the *miniSINEUP-Sox9* constructs containing m5C, Ψ, or N1mΨ; *miniSINEUP-Sox9* contains an overlapping region with *Sox9* mRNA as a BD and the SINEB2 element as an ED. (B) Translational upregulation of SOX9 after transfection of mIVT SINEUP RNAs. Images shown are representative western blots illustrating the effect of mIVT SINEUPs on the SOX9 protein level. Quantification of SOX9 levels compared with nontransfected cells (Cont.) is shown as means ± SD of at least 3 independent experiments. **$P < 0.01$; ns, not significant (two-tailed Student's *t*-test). (C) Quantification of *Sox9* mRNA and miniSINEUP RNA levels after transfection of mIVT SINEUPs. ns, not significant (two-tailed Student's *t*-test). Data are shown as means ± SD from at least three independent experiments.

therapies and, thus, would benefit patients with diseases that are currently difficult to treat by using conventional treatments including DNA-based gene therapy.

Conflicts of interest

SZ, SG, and PC are inventors on patent US9353370B2 and related applications in the European Union and Japan, and HT, SZ, SG, and PC are inventors on patent application IT02018000002411 and the related application PCT/IB2019/050914, which is held by SISSA and TranSINE Therapeutics (Cambridge, UK), which was founded by SG and PC and in which HT owns shares. These COIs did not affect the direction and conclusions of this paper.

Author contributions

NT, HT, and PC designed the project with input from SZ and SG; NT performed all experiments and data analysis; and NT, HT, and PC wrote the manuscript with input from SZ and SG.

References

1 Mattick JS and Makunin IV (2006) Non-coding RNA. *Hum Mol Genet* **15**, R17–R29.

2 Carninci P, Kasukawa T, Katayama S, Gough J, Frith MC, Maeda N, Oyama R, Ravasi T, Lenhard B, Wells C *et al.* (2005) The transcriptional landscape of the mammalian genome. *Science* **309**, 1559–1563.

3 ENCODE Project Consortium (2012) An integrated encyclopedia of DNA elements in the human genome. *Nature* **489**, 57–74.

4 Slack FJ and Chinnaiyan AM (2019) The role of non-coding RNAs in oncology. *Cell* **179**, 1033–1055.

5 Zucchelli S, Fedele S, Vatta P, Calligaris R, Heutink P, Rizzu P, Itoh M, Persichetti F, Santoro C, Kawaji H *et al.* (2019) Antisense transcription in loci associated to hereditary neurodegenerative diseases. *Mol Neurobiol* **56**, 5392–5415.

6 Carrieri C, Cimatti L, Biagioli M, Beugnet A, Zucchelli S, Fedele S, Pesce E, Ferrer I, Collavin L, Santoro C *et al.* (2012) Long non-coding antisense RNA controls Uchl1 translation through an embedded SINEB2 repeat. *Nature* **491**, 454–457.

7 Zucchelli S, Fasolo F, Russo R, Cimatti L, Patrucco L, Takahashi H, Jones MH, Santoro C, Sblattero D, Cotella D *et al.* (2015) SINEUPs are modular antisense long non-coding RNAs that increase synthesis of target proteins in cells. *Front Cell Neurosci* **9**, 174.

8 Schein A, Zucchelli S, Kauppinen S, Gustincich S and Carninci P (2016) Identification of antisense long noncoding RNAs that function as SINEUPs in human cells. *Sci Rep* **6**, 33605.

9 Patrucco L, Chiesa A, Soluri MF, Fasolo F, Takahashi H, Carninci P, Zucchelli S, Santoro C, Gustincich S, Sblattero D *et al.* (2015) Engineering mammalian cell factories with SINEUP noncoding RNAs to improve translation of secreted proteins. *Gene* **569**, 287–293.

10 Espinoza S, Scarpato M, Damiani D, Manago F, Mereu M, Contestabile A, Peruzzo O, Carninci P, Santoro C, Papaleo F *et al.* (2019) SINEUP Non-coding RNA targeting GDNF rescues motor deficits and neurodegeneration in a mouse model of Parkinson's disease. *Mol Ther* **28**, 642–652.

11 Bon C, Luffarelli R, Russo R, Fortuni S, Pierattini B, Santulli C, Fimiani C, Persichetti F, Cotella D, Mallamaci A *et al.* (2019) SINEUP non-coding RNAs rescue defective frataxin expression and activity in a cellular model of Friedreich's Ataxia. *Nucleic Acids Res* **47**, 10728–10743.

12 Indrieri A, Grimaldi C, Zucchelli S, Tammaro R, Gustincich S and Franco B (2016) Synthetic long non-coding RNAs [SINEUPs] rescue defective gene expression *in vivo*. *Sci Rep* **6**, 27315.

13 Takahashi H and Carninci P (2014) Widespread genome transcription: new possibilities for RNA therapies. *Biochem Biophy Res Commun* **452**, 294–301.

14 Gustincich S, Zucchelli S and Mallamaci A (2017) The Yin and Yang of nucleic acid-based therapy in the brain. *Prog Neurogibol* **155**, 194–211.

15 Dang VT, Kassahn KS, Marcos AE and Ragan MA (2008) Identification of human haploinsufficient genes and their genomic proximity to segmental duplications. *Eur J Hum Genet* **16**, 1350–1357.

16 Lek M, Karczewski KJ, Minikel EV, Samocha KE, Banks E, Fennell T, O'Donnell-Luria AH, Ware JS, Hill AJ, Cummings BB *et al.* (2016) Analysis of protein-coding genetic variation in 60,706 humans. *Nature* **536**, 285–291.

17 Toki N, Takahashi H, Zucchelli S, Gustincich S and Carninci P (2019) SINEUP long non-coding RNA acts via PTBP1 and HNRNPK to promote translational initiation assemblies. *bioRxiv* 664029 [PREPRINT].

18 Takahashi H, Kozhuharova A, Sharma H, Hirose M, Ohyama T, Fasolo F, Yamazaki T, Cotella D, Santoro C, Zucchelli S *et al.* (2018) Identification of functional features of synthetic SINEUPs, antisense lncRNAs that specifically enhance protein translation. *PLoS One* **13**, e0183229.

19 Mandal PK and Rossi DJ (2013) Reprogramming human fibroblasts to pluripotency using modified mRNA. *Nat Protoc* **8**, 568–582.

20 Amort T, Rieder D, Wille A, Khokhlova-Cubberley D, Riml C, Trixl L, Jia X-Y, Micura R and Lusser A (2017) Distinct 5-methylcytosine profiles in poly(A) RNA from mouse embryonic stem cells and brain. *Genome Biol* **18**, 1.

21 Trixl L and Lusser A (2019) The dynamic RNA modification 5-methylcytosine and its emerging role as an epitranscriptomic mark. *Wiley Interdiscip Rev RNA* **10**, e1510.

22 Kierzek E, Malgowska M, Lisowiec J, Turner DH, Gdaniec Z and Kierzek R (2014) The contribution of pseudouridine to stabilities and structure of RNAs. *Nucleic Acids Res* **42**, 3492–3501.

23 Anderson BR, Muramatsu H, Nallagatla SR, Bevilacqua PC, Sansing LH, Weissman D and Kariko K (2010) Incorporation of pseudouridine into mRNA enhances translation by diminishing PKR activation. *Nucleic Acids Res* **38**, 5884–5892.

24 Svitkin YV, Cheng YM, Chakraborty T, Presnyak V, John M and Sonenberg N (2017) N1-methyl-pseudouridine in mRNA enhances translation through eIF2alpha-dependent and independent mechanisms by increasing ribosome density. *Nucleic Acids Res* **45**, 6023–6036.

25 Andries O, Mc Cafferty S, De Smedt SC, Weiss R, Sanders NN and Kitada T (2015) N(1)-methylpseudouridine-incorporated mRNA outperforms pseudouridine-incorporated mRNA by providing enhanced protein expression and reduced immunogenicity in mammalian cell lines and mice. *J Control Release* **217**, 337–344.

26 Mauger DM, Cabral BJ, Presnyak V, Su SV, Reid DW, Goodman B, Link K, Khatwani N, Reynders J, Moore MJ *et al.* (2019) mRNA structure regulates protein expression through changes in functional half-life. *Proc Natl Acad Sci USA* **116**, 24075–24083.

27 Symon A and Harley V (2017) SOX9: A genomic view of tissue specific expression and action. *Int J Biochem Cell Biol* **87**, 18–22.

28 Font-Burgada J, Shalapour S, Ramaswamy S, Hsueh B, Rossell D, Umemura A, Taniguchi K, Nakagawa H, Valasek MA, Ye L *et al.* (2015) Hybrid periportal hepatocytes regenerate the injured liver without giving rise to cancer. *Cell* **162**, 766–779.

29 Furuyama K, Kawaguchi Y, Akiyama H, Horiguchi M, Kodama S, Kuhara T, Hosokawa S, Elbahrawy A, Soeda T, Koizumi M *et al.* (2011) Continuous cell supply from a Sox9-expressing progenitor zone in adult liver, exocrine pancreas and intestine. *Nat Genet* **43**, 34–41.

30 Alexandrov A, Chernyakov I, Gu W, Hiley SL, Hughes TR, Grayhack EJ and Phizicky EM (2006) Rapid tRNA decay can result from lack of nonessential modifications. *Mol Cell* **21**, 87–96.

31 Hussain S, Sajini AA, Blanco S, Dietmann S, Lombard P, Sugimoto Y, Paramor M, Gleeson JG, Odom DT, Ule J *et al.* (2013) NSun2-mediated cytosine-5 methylation of vault noncoding RNA determines its processing into regulatory small RNAs. *Cell Rep* **4**, 255–261.

32 Yang X, Yang Y, Sun B-F, Chen Y-S, Xu J-W, Lai W-Y, Li A, Wang X, Bhattarai DP, Xiao W *et al.* (2017) 5-methylcytosine promotes mRNA export - NSUN2 as the methyltransferase and ALYREF as an m(5)C reader. *Cell Res* **27**, 606–625.

33 Amort T, Souliere MF, Wille A, Jia X-Y, Fiegl H, Worle H, Micura R and Lusser A (2013) Long non-coding RNAs as targets for cytosine methylation. *RNA Biol* **10**, 1003–1008.

34 Roundtree IA, Evans ME, Pan T and He C (2017) Dynamic RNA modifications in gene expression regulation. *Cell* **169**, 1187–1200.

35 Baudin-Baillieu A, Fabret C, Liang X-H, Piekna-Przybylska D, Fournier MJ and Rousset J-P (2009) Nucleotide modifications in three functionally important regions of the Saccharomyces cerevisiae ribosome affect translation accuracy. *Nucleic Acids Res* **37**, 7665–7677.

36 Kallen K-J and Thess A (2014) A development that may evolve into a revolution in medicine: mRNA as the basis for novel, nucleotide-based vaccines and drugs. *Ther Adv Vaccines* **2**, 10–31.

37 Zucchelli S, Cotella D, Takahashi H, Carrieri C, Cimatti L, Fasolo F, Jones MH, Sblattero D, Sanges R, Santoro C *et al.* (2015) SINEUPs: A new class of natural and synthetic antisense long non-coding RNAs that activate translation. *RNA Biol* **12**, 771–779.

38 Sasso E, Latino D, Froechlich G, Succoio M, Passariello M, De Lorenzo C, Nicosia A and Zambrano N (2018) A long non-coding SINEUP RNA boosts semi-stable production of fully human monoclonal antibodies in HEK293E cells. *mAbs* **10**, 730–737.

39 Bailey JK, Shen W, Liang X-H and Crooke ST (2017) Nucleic acid binding proteins affect the subcellular distribution of phosphorothioate antisense oligonucleotides. *Nucleic Acids Res* **45**, 10649–10671.

Supporting information

Additional supporting information may be found online in the Supporting Information section at the end of the article.

Fig. S1. (A) Schematic diagram of the multicloning region in pCS2+. (B) *miniSINEUP-Sox9* construct. The SINEUP targeting mouse Sox9 consists of a BD that overlaps the *Sox9* mRNA sequence and an ED containing an inverted SINEB2 sequence from mouse *AS-Uchl1* RNA. The SINEUP was cloned into the XhoI and XbaI sites of pCS2+ (A). Underlining highlights BD of *Sox9* mRNA; ED is italicized, and restriction sites are in red (XhoI, CTCGAG; XbaI, TCTAGA).

Fig. S2. (A) Quantification of *EGFP* mRNA levels after co-transfection of pEGFP-C2 plasmid and each transcribed SINEUP. ns, not significant (two-tailed Student's *t*-test). Data are shown as means $\pm$ SD from at least three independent experiments. (B) Quantification of SINEUP RNA levels after co-transfection of pEGFP-C2 plasmid and each transcribed SINEUP. $**P < 0.01$; $*P < 0.05$; ns, not significant (two-tailed Student's *t*-test). Data are shown as means $\pm$ SD from at least three independent experiments.

Fig. S3. (A) Subcellular distribution of mIVT SINEUP RNAs in cells transfected with mIVT SINEUP RNAs alone. Bar, 5 μm. (B) Subcellular distribution of *EGFP* mRNA in cells transfected with pEGFP-C2 plasmid alone. Bar, 5 μm.

Fig. S4. (A–C) SINEUP RBPs in HepG2, Hepa 1–6, and HEK293T/17 cells. Images shown are representative Western blots of (A) the RBPs in HepG2 and Hepa 1–6 cell lysates compared with HEK293T/17 cell lysate. The protein levels of the SINEUP RBPs (B) PTBP1 and (C) HNRNPK were normalized to that of β-actin. Fold change in the protein levels is shown as means $\pm$ SD of at least three independent experiments. $***P < 0.001$, ns, not significant (two-tailed Student's *t*-test).

Table S1. FISH probe sequences for SINEUP RNAs.
Table S2. FISH probe sequences for *EGFP* mRNAs.